Eur. Phys. J. D **16**, 321–324 (2001)

THE EUROPEAN PHYSICAL JOURNAL D

EDP Sciences

Second harmonic generation in Ga nanoparticle monolayers

A.M. Malvezzi[1,a], M. Patrini[2], A. Stella[2], P. Tognini[2], P. Cheyssac[3], and R. Kofman[3]

[1] INFM - Dip. Elettronica, Università di Pavia, Via Ferrata 1, I-27100 Pavia, Italy
[2] INFM - Dip. Fisica "A. Volta" Università di Pavia, Via Bassi 6, I-27100 Pavia, Italy
[3] Laboratoire de la Physique de la Matière Condensée, Université de Nice Sophia Antipolis, 06108 Nice Cedex, France

Received 29 November 2000

Abstract. Ga nanoparticle monolayers formed by evaporation-condensation in ultrahigh vacuum and embedded in a transparent SiO_x matrix generate second harmonic (SH) signals in transmission and reflection when illuminated by a 150 fs, 800 nm laser pulses. The observed SH light exhibits a critical dependence on input and output polarizations, angle of incidence and azimuthal orientation of the samples. The results lead to a consistent picture of shape and orientation of the nanoparticles. Linear transmittance spectra in the visible range support these findings and the observed size dependence of the SH signal.

PACS. 78.66.Vs Fine-particle systems – 61.25.Mv Liquid metals and alloys – 42.65.Ky Harmonic generation, frequency conversion

1 Introduction

Nonlinear optical properties of nanostructured materials are being intensively studied in view of device development in many photonic applications. The importance of the field is based on the possibility of manipulating such structures on a nanoscopic level and integrating them on already existing electro-optical devices [1,2]. A desirable feature of these materials is the achievement of high efficiency nonlinear signal conversion even with low symmetry structures grown with self-assembled procedures [3].

In this work, the second harmonic (SH) response induced by fs laser pulses on Ga nanoparticles is studied and related to the optical linear response measured in transmission and to the structure of the samples. Measurements were performed by varying nanoparticle size, laser fluence, polarization of the exciting pulse and geometry of the experiment. Both nonlinear reflectivity and transmission measurements were performed. We have measured substantial amounts of second harmonic radiation generated by Ga nanoparticles. Moreover, our results stress the importance of second harmonic generation as a viable and sensitive tool for nanoscopic studies and characterization of these structures.

2 Experimental details

The particles are formed by evaporation-condensation (Vollmer - Weber mode) of high purity gallium in ultrahigh vacuum on a dielectric SiO_x ($x \sim 1$) layer deposited on a silica or sapphire substrate [4]. The system is then covered with a layer of the same material, with a thickness ranging from 10 to 50 nm.

The nanoparticles are produced on a single layer as truncated spheres (80% of the ideal volume) with a relatively low ($\leq$ 20%) size dispersion. The Ga nanoparticles are in the liquid phase at room temperature. In our samples, they have an equivalent mass thickness d_M of 1, 2, 3, 5, 10, 20 and 30 nm, and are labelled Ga1, Ga2, Ga3, Ga5, Ga10, Ga20, Ga30 hereafter. The equivalent mass thickness is defined as the thickness of the layer that would be formed if the evaporated material were uniformly distributed on the surface. The corresponding value of the mean radius of the particles was estimated by transmission electron microscopy (TEM) measurements on co-evaporated samples and was about twice d_M [5].

Linear transmittance (T) spectra at room temperature and at near-normal incidence were measured by a Varian Cary 5E spectrophotometer in the wavelength range 0.3-3 μm, with step of 1 nm. The spectral bandwidth (SBW) is 3 nm. For the typical value $T = 0.5$, the absolute accuracy in T is better than 1.5×10^{-3} and the repeatability in T is about 1.5×10^{-4}.

Second-harmonic generation was measured in transmission and reflection with a femtosecond Ti:sapphire laser at 800 nm, repetition rate 1 kHz, pulse duration 150 fs. The maximum pulse fluence on sample is 5×10^{-3} J/cm^2 at the 0.9 mm diameter focal spot of the 4-m focussing lens used in the experiment. The SH signal is detected by a photomultiplier, after passing through a combination of color glass and interference filters to suppress the fundamental radiation.

[a] e-mail: malvezzi@ele.unipv.it

3 Results and discussion

Linear transmittance spectra of all samples from Ga1 to Ga30 are shown in Fig. 1, where the arrow indicates increasing d_M values. The spectra of the sapphire substrate alone (dashed line) and covered with the SiO_x layer (dotted line) are also shown. The dominant feature is the absorption contribution from the surface plasma resonance, which increases and broadens with increasing particle size. In the Maxwell-Garnett effective-medium approach for the layer composed by nanoparticles and matrix the energy position of the plasma resonance peak equals $\omega_p/(1+2\varepsilon_m)^{1/2}$, where ω_p is the bulk plasma resonance of Ga (about 14 eV) and ε_m is the real part of the dielectric function of the matrix material. The FWHM of the resonance is size-dependent and is inversely proportional to the momentum relaxation time of conduction electrons which decreases with particle size.

The quantitative analysis of these spectra has been developed in [5]. Here we only focus on the following features: a) the surface plasmon resonance peak falls at our second-harmonic wavelength (400 nm) for Ga thickness values d_M between 10 and 20 nm; b) the azimuthal rotation ϕ of the samples around their surface normal produces a slight oscillation in the T values, with a 180 degree period and about 5% amplitude.

Absolute calibration of the measured SH values was obtained by taking into account geometry, optical characteristics of our experimental setup and detector sensitivity. The SH signals detected both in reflection and transmission follow a quadratic law in the input fluence. The nonlinear radiation appears to be spatially coincident with the pump in reflection and transmission. This has been verified using a diaphragm in front of the detector. Fig. 2, for example, illustrates the transmitted SH signal from sample Ga10 *versus* laser intensity.

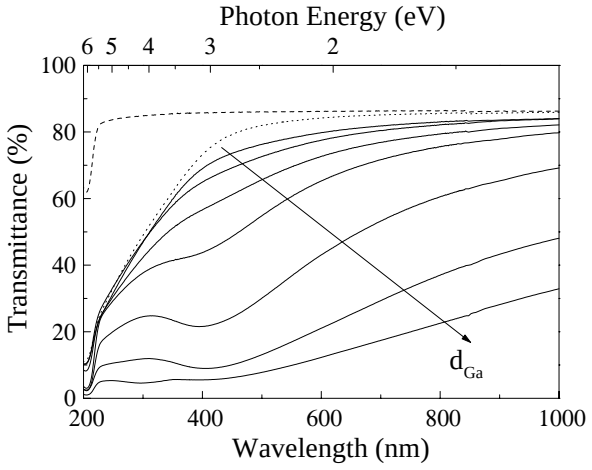

Fig. 1. Linear transmittance spectra of the Ga nanoparticle samples: the arrow indicates increasing d_M values from 1 to 30 nm. The dashed line refers to the sapphire substrate and the dotted one to the substrate covered with a 50 nm SiO_x layer.

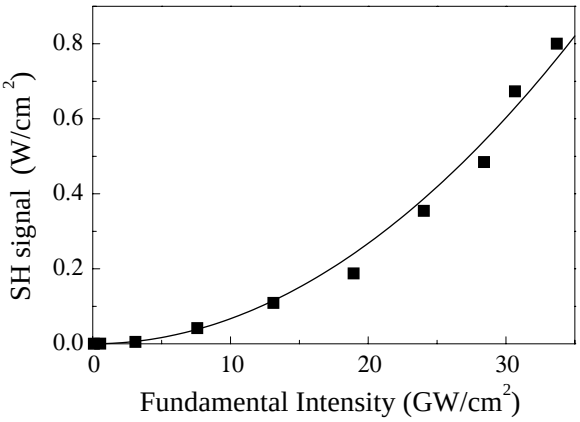

Fig. 2. Transmitted SH signal *versus* fundamental intensity for sample Ga10.

For a quantitative comparison of the SH generation efficiency, we have measured on the same apparatus the nonlinear reflectivity of crystalline GaAs(100) and Si(100) surfaces, obtaining SH values of $\approx 10^{-26}$ and $\approx 10^{-22}$ m^2/W, respectively. The maximum nonlinear reflectivity of our Ga samples lays in between these values, *i.e.* $\approx 2.5 \times 10^{-25}$ m^2/W.

Nonlinear reflection and transmission measurements were performed on several sets of Ga nanoparticle samples at variable fluence levels. The data were collected at normal incidence in transmission and at 2 degrees in reflection. Substrate samples, as well as substrates covered with SiO_x layers, have shown negligible SH generation both in reflection and transmission. Nonlinear transmission measurements have been performed by both varying the azimuthal angle ϕ at normal incidence and the incidence angle θ at fixed azimuth.

Fig. 3 summarizes the measurements of nonlinear transmission *versus* the azimuthal angle ϕ with fixed input linear polarization and for different equivalent monolayer thicknesses d_M. All samples exhibit the same $\sin^2\phi$ dependence, where the zero in angle ϕ refers to a fixed orientation of substrates in the deposition chamber. Note that the maximum values rise above the minima up to a factor of eight. When input circular polarization is applied, instead, the observed oscillations are strongly reduced, due to the compensation of two mutually perpendicular linear polarizations.

This behavior was observed also in reflection with input linear polarization. Typical results are shown in Fig. 4. Note that maxima and minima occur at the same azimuthal angles as in transmission.

It is well known that for an isotropic active layer the SH signal is negligible at normal incidence in reflection and transmission [6,7]. The very presence of a SH signal at normal incidence unambiguously reveals a broken surface symmetry induced by the nanoparticle monolayers. Moreover, the 180 degree modulation of the SH signal observed in linear polarization indicates an anisotropic structure of the nanoparticle network. This behaviour is suggestive of

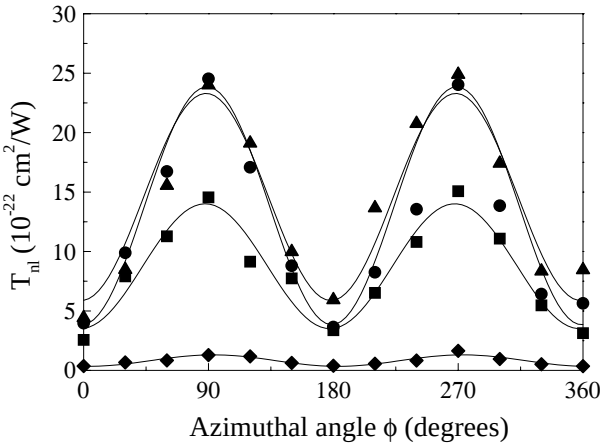

Fig. 3. Nonlinear transmission *versus* azimuthal angle for samples with different Ga equivalent thickness: d_M = 3 nm (diamonds), 10 nm (circles), 20 nm (triangles) and 30 nm (squares).

oblate nanoparticles with a preferred orientation on the surface.

Further insight can be gained by monitoring the nonlinear transmission intensity at a fixed azimuth angle by varying the angle of incidence θ of the radiation on the sample surface. In this case, one explores the symmetry of the layer around the surface axis perpendicular to the incidence plane.

The SH signals have been also analyzed in polarization and in the following are labelled as T_{nl}^{xy} with x (y) referring to input (output) polarizations. In Fig. 5, for example, the nonlinear transmissions T_{nl}^{pp} and T_{nl}^{ps} measured at fixed azimuthal angle (90 degrees) are shown as a function of the incident angle θ for the Ga20 sample. The T_{nl}^{pp} measurements give rise to a quasi-parabolic dependence on θ in the range explored. The T_{nl}^{ps} measurements exhibit the same quasi-parabolic dependence but the enhancement at large angles is negligible with respect to T_{nl}^{pp}. The same negligible SH signal is observed with the reference sample (matrix layer on substrate). The strong angular dependence of T_{nl}^{pp} is a general trend of metallic materials with high linear dielectric functions and has been described in Ref. [6].

On the other hand, the input s-polarization response is found to be almost negligible. We have checked that the output SH signal in this case is completely p-polarized, *i.e.* $T_{nl}^{ss} \approx 0$. This result is in line with the quasi continuous character of our nanoparticle monolayers. Indeed, for a continuous film T_{nl}^{ss} is exactly zero at all incidence angles [8].

Moreover, it is found that $T_{nl}^{sp} \approx T_{nl}^{ps}$. This means that the second order susceptibility $\chi^{(2)}$ has extra off-diagonal components.

In Figure 6, T_{nl}^{p} for three different samples is illustrated as a function of the angle of incidence. Here, a further observation is the angular position of the minimum which varies with the nanoparticle size and shifts towards zero with increasing d_M. This can be interpreted as an indication of a non-symmetric positioning of nonspherical particles on the sample surface. In this respect, for example, the major symmetry axis of the nanoparticles in Ga5 sample appears misaligned with respect to the surface plane of about 13 degrees.

Note that the T_{nl} values measured at normal incidence are coincident with those reported in Fig. 3 for $\phi = 90°$.

The intensity of SH signals in reflection and transmission is strongly dependent on particle size. They have approximately the same dependence and reach comparable values. Both intensity measurements exhibit a broad maximum occurring for d_M values between 10 and 20 nm. The corresponding surface plasmon frequency is resonant with the SH frequency, suggesting a dominance of surface generation mechanisms over bulk higher order contributions.

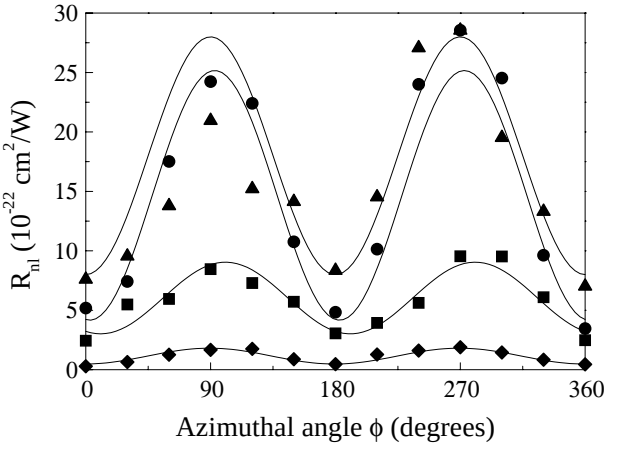

Fig. 4. Nonlinear reflection *versus* azimuthal angle for samples with different Ga equivalent thickness: d_M =3 nm (diamonds), 10 nm (circles), 20 nm (triangles) and 30 nm (squares).

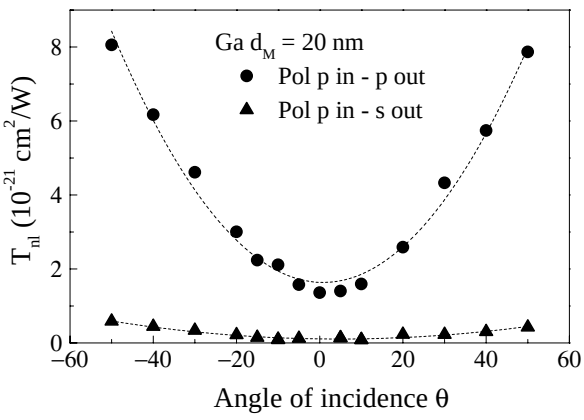

Fig. 5. Nonlinear transmission of Ga20 sample *versus* angle of incidence and with azimuth angle ϕ = 90 degrees with the input/output polarizations indicated.

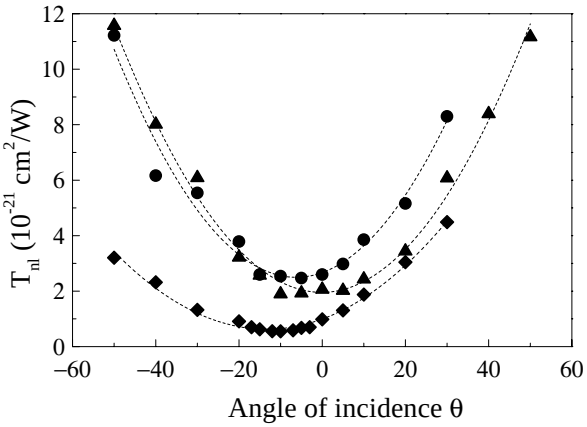

Fig. 6. Nonlinear transmission *versus* angle of incidence for different samples for input p-polarization and azimuth angle $\phi = 90$ degrees: $d_M = 5$ nm (diamonds), 10 nm (circles), 20 nm (triangles).

4 Conclusions

In this paper we have investigated the SH response of Ga liquid nanoparticles using fs laser pulses. Nonlinear reflection and transmission coefficients have been evaluated for several geometrical and polarization configurations. These measurements are suggestive of asymmetric shapes but correlated orientation of the nanoparticles. The same observations could not be deduced from linear transmittance measurements. Only in few selected samples a slight azimuthal dependence of the transmittance has been barely observed.

The body of SH observations is self-consistent and leads to the notion of a statistically preferred orientation of prolate Ga nanoclusters with the symmetry axis slightly departing from the sample plane. The observations also reproduce themselves from sample to sample, irrespective of the substrate material. This points towards the specific growth technique used as the principal responsible of this anomaly. Work is in progress to further elucidate this point.

These investigations demonstrate the extreme sensitivity of SH techniques in the determination of nanocluster monolayer geometry and layout. The dependence of SH signal on particle shape is also suggestive of a dominant surface contribution to the SH signal. This can be ascribed to local symmetry breaking due to a) particle shape asymmetries and b) statistical fluctuations of particle size and orientation [3].

The laser source was kindly made available by INFM-Project (PRA) "Elphos". We also acknowledge financial support from Progetto Finalizzato Materiali e Dispositivi per l'Elettronica dello Stato Solido II (MADESS II) of CNR and from Progetto di Ateneo "Nuovi materiali nanostrutturati" by the University of Pavia.

References

1. B.J. Seller, D.G. Hall, Opt. Lett. **25**, 1071 (2000).
2. A. Brysch, G. Bour, R. Neuendorf, U. Kreibig, Appl. Phys. B **68**, 447 (1999).
3. O.A. Aktsipetrov, P.V. Alyutin, A.A. Fedyanin, A.A. Niculin, A.N. Rubtsov, Surf. Sci. **325**, 343 (1995).
4. E. Sondergard, R. Kofman, P. Cheyssac, A. Stella, Surf. Sci. **364**, 467 (1996).
5. P. Tognini, A. Stella, P. Cheyssac, R. Kofman, J. Non-Cryst. Solids **249**, 117 (1999).
6. N. Bloembergen, R.K. Chang, S.S. Jha, C.H. Lee, Phys. Rev. B **174**, 813 (1968).
7. Y.R. Shen, *The Principles of Nonlinear Optics* (Wiley, New York, 1984).
8. V. Mizrahi, J.E. Sipe, J. Opt. Soc. Am. B **5**, 660 (1988).